Femtosecond time-resolved thermomodulation of thin gold films with different crystal structures

H. E. Elsayed-Ali*
Laboratory for Laser Energetics, University of Rochester, 250 East River Road, Rochester, New York 14623-1299

T. Juhasz
Department of Physics, University of California, Irvine, California 92717
(Received 6 May 1992)

A femtosecond laser is used to generate and probe hot electrons in polycrystalline and single-crystalline thin gold films. Transient thermoreflectivity and thermotransmissivity for different heating-laser-pulse fluences are performed. Analysis of the transient thermotransmissivity and thermoreflectivity signals allows us to resolve the modulation to the real and the imaginary parts of the dielectric constant. The latter is found to be dominant at our probe wavelength. The hot-electron energy-loss lifetime is shown to be 1–3 ps and increases with the laser fluence. For film thickness comparable to the optical skin depth, the transient decay time of the reflectivity and of the transmissivity are equal, with the polycrystalline films showing a slightly faster decay time. For thicker films, hot-electron transport to the bulk of the film gives a faster transient-reflectivity decay. Electron transport is slower in the polycrystalline films.

I. INTRODUCTION

The use of ultrafast lasers to generate nonequilibrium heating conditions in metals was suggested many years ago.[1] If a metal is subjected to pulsed-laser heating for which the pulse duration is less than or comparable to hot-electron energy-loss lifetime, then a transient inequality between the effective temperatures of the electrons and the lattice would occur. Nonequilibrium heating in metals is not limited to ultrafast laser heating. It is a general phenomenon that can occur when the electron gas in the metal is subjected to a transient event, such as picosecond for femtosecond laser heating, a fast electric current, or the slowing down of energetic charged particles. In fact, one of the earliest theoretical studies[2] of hot-electron generation and relaxation in metals was primarily concerned with the generation of these nonequilibrium conditions during the slowing down of energetic charged particles in metals.

Hot-electron energy-loss lifetime in metals, $\tau_{e\text{-ph}}$, can vary greatly depending on the initial ambient temperature. At low temperatures, only low-energy acoustic phonons are available to interact with the hot electrons; and since the corresponding phonon density of states is small, the coupling of the electron gas to the phonons is weak. This results in an electron energy-loss lifetime on the order of 1 ms for copper at 25 mK.[3] At higher temperatures, $\tau_{e\text{-ph}}$ is significantly reduced and at tens of degrees kelvin can be as short as a few picoseconds.[4,5] Such extremely fast energy-loss lifetime have made the observation of nonequilibrium heating, in this region, inaccessible except with the use of ultrafast duration pulsed lasers. Moreover, the generation of a significant (up to a few thousand of degrees) difference between the effective electron and lattice temperatures is demonstrated only by the use of ultrafast lasers.[5–10]

Nonequilibrium electron heating in metals has been observed by ultrafast time-resolved thermomodulation reflectivity and transmissivity,[4–8] thermally assisted multiphoton photoemission,[9] and more recently single-photon photoemission.[10] Femtosecond thermomodulation studies have demonstrated the fast nature of hot-electron relaxation by energy loss in geometrically confined films (with thickness comparable to the laser skin depth) and by energy loss and transport in thicker films. Subsequently, surface-plasmon resonance in thin silver films has been shown to provide a very sensitive probe of nonequilibrium heating.[11] A systematic study of electron-phonon coupling in different thin metal films was conducted.[12] In this later study, a very thin copper film deposited on the various metal films was used as a hot-electron probe, thus facilitating the study of hot-electron relaxation in different metals. Results were in agreement with a theoretical model of electron-phonon coupling.[13] A thermomodulation study of electron-phonon relaxation in niobium was performed by observing the rate of lattice heating due to energy transfer from the hot electrons.[14] An approach to measuring electron-phonon coupling in metals based on a comparison of the experimental damage threshold for different laser pulse widths with a heat transport model was previously proposed.[15] However, some concerns regarding its implementation was subsequently commented on.[16] In these studies the role of lattice imperfections on hot-electron energy loss and transport was not considered. Nonequilibrium heating by femtosecond lasers has also been shown to strongly affect the desorption kinetics of molecular adsorbates on metal substrates.[17] In this case the desorption yield was described by that expected from coupling to the adsorbate of the substrate's nonequilibrium electrons, which are at a significantly higher temperature than that of the lattice.[18]

We have conducted a set of pump-probe experiments on thin (100–800 Å) single-crystalline and polycrystalline

gold films. An earlier account of our results was previously given.[19] Here we detail our results and extend our analysis of the thermomodulation data. Both femtosecond time-resolved thermoreflectivity and thermotransmissivity were observed. Reflectivity and transmissivity are complimentary in the sense that the reflectivity probes a depth comparable to the skin depth of the laser in gold ($\sim$150 Å), whereas the transmissivity probes the total thickness of the film. Moreover, for a uniformly heated film (when the thickness is less than or comparable to the laser skin depth), the combined transient reflectivity and transmissivity, along with the known thickness of the film and the index of refraction of the substrate, is sufficient to determine transient changes in the real and imaginary parts of the dielectric constant (ε_1 and ε_2, respectively). Our results show that, for film thickness comparable to the skin depth, the decay time of the transient reflectivity is equal to that of the transmissivity. This occurs in both single-crystalline and polycrystalline films. For thicker films, hot-electron transport inside the film gives a faster transient reflectivity decay. Transient transmissivity decay time is less affected by the increased film thickness. Comparison of data using single-crystalline films to those using polycrystalline films indicates that electron transport is impeded by the predominantly elastic electron-grain boundary collisions.

II. EXPERIMENT

The polycrystalline gold films were deposited on a glass slide by conventional resistive evaporation techniques. The film thickness was determined by a crystal thickness monitor with an estimated accuracy of better than $\pm$50 Å for the 200-Å films. Electron diffraction patterns obtained from films deposited, under the same deposition conditions, on formvar supported on a standard copper electron microscope grid show a ring pattern. TEM images reveal a grain size on the order of a few hundred angstroms. Single-crystalline thin gold films were also fabricated by evaporation. For these films, however, we used a sodium chloride crystal as a substrate. To fabricate the single crystals, the substrate was heated to $\sim$600 K then allowed to cool to $\sim$450 K. A very thin layer ($<$20 Å) of silver was initially deposited at a rate of $\sim$1 Å/s. This serves to enhance the epitaxy of the subsequently deposited gold. After deposition of the gold film at $\sim$450 K, at a rate of a few angstroms per second, the substrate was allowed to cool under vacuum then removed from the evaporator. The film was floated on distilled water, washed in sulphuric acid to remove the silver and any gold-silver alloy that might have formed in the interface, and then washed again in distilled water. Finally, the film was caught on a glass slide and allowed to dry.

Electron diffraction patterns obtained from the epitaxially grown films show a spot pattern consistent with a single crystal oriented in the (100) orientation. Transmission electron microscope images reveal oriented grains characteristic of epitaxially grown thin metal films. Electron diffraction patterns and electron micrographs of polycrystalline and single-crystalline 400-Å gold films are shown in Fig. 1. A very high density ($>10^{10}$ cm^{-2}) of dislocations and twins are evident in the electron micrographs of the single-crystalline films. Such a high density of dislocations and twins is characteristic of these single-crystalline films.[20] From Fig. 1, the grain size for the polycrystalline samples can be estimated to be in the order of a few hundred angstroms. More quantitative surface grain size determination was accomplished using atomic force microscopy with an image analysis system. Images were obtained for both types of samples in air. The average grain size of a typical 200-Å polycrystalline film was determined to be 155$\pm$10 Å. No systematic study of the dependence of the average grain size on film thickness was conducted. Atomic force microscope images of the 200-Å single-crystalline film showed oriented crystallites connected by bridges. Contrary to the polycrystalline films, obtaining atomic resolution on the single-crystalline film was possible. This seems to be consistent with the assumption of relative flatness of the epitaxially grown films, which has previously been concluded based on the observation of streaks in reflection high-energy electron diffraction patterns.[21]

The pump-probe experiments were performed with the use of a 76-MHz synchronously pumped linear-cavity femtosecond dye laser.[22] Intracavity control of the group velocity dispersion is accomplished using Brewster-angle prisms. This system delivered $\sim$150 fs (sech^2) pulses at $\sim$615-nm wavelength (2-eV photon energy). A maximum pulse energy of $\sim$0.6 nJ can be achieved. The laser is actively stabilized to achieve a stability of the frequency spectrum and pulse width for several hours. A conventional pump-probe setup was used. The probe beam was delayed from the pump using a stepper motor with 1-μm resolution. Both pump and probe were incident on the sample at near normal incidence with their focal spot on the sample 5$\pm$1 μm as measured with a scanning blade. A 10$\times$ microscope objective was used for focusing. The probe energy was fixed while the pump was varied using neutral density filters. The pump-to-probe energy was maintained higher than a factor of 17. The pump was modulated with either a mechanical chopper or an acousto-optic modulator and the thermomodulation signal was detected using a lock-in amplifier tuned to the pump chopping frequency.

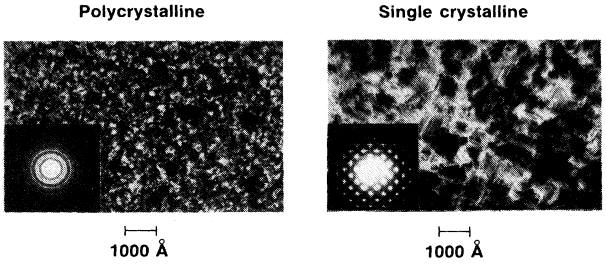

FIG. 1. Transmission electron micrographs and electron diffraction patterns of polycrystalline and single-crystalline gold films.

III. FEMTOSECOND THERMOMODULATION

For metals, heating-induced modulation of their optical properties can result from many effects. Of particular importance to thermomodulation studies is the change in the occupancy of electronic states near the Fermi level.[23] The top of the d band to the Fermi level in Au is at ~ 2.4 eV.[24] Therefore, there are allowed transitions from the top of the d band to states near the Fermi level for a wavelength near that of the laser system used in the present study ($\lambda = 615$ nm). The electronic-heating-induced smearing of the Fermi distribution affects the complex dielectric constant (a function of wavelength) of the metal, thus modulating its optical properties. While our laser photon energy is lower than that of the interband edge, thermomodulation measurements,[25] and relativistic band calculations[26] of the optical properties of gold are in agreement on the existence of an absorption tail below the interband edge, which is due to band structure. This edge extends as low as 1.7 eV.[25] While the magnitude of the thermomodulation signal is significantly reduced at our laser wavelength compared to that near the interband edge, the signal we obtain is well within our detection limit.

Time-resolved thermotransmissivity signals of 200-Å single-crystalline gold film taken with two different laser heating fluences are shown in Fig. 2. The shape of these signals is very similar to those observed for thermoreflectivity for the 200-Å films. These signals consist of a fast initial modulation related to the heating laser pulse width, a transient fast decay occurring in a 1–3 ps time scale, and a subsequent long tail persisting for times that appear to be much longer than our probing time. The general shape of these signals is similar to those observed for other gold film thicknesses. The temporal evolution of the fast transient appears to be exponential for all laser fluences as shown by plotting it on a semilogarithmic plot. Both thermoreflectivity and thermotransmissivity ($\Delta R/R$ and $\Delta T/T$) are negative at the probe wavelength. The transient thermomodulation signal appears to be directly proportional to the heating laser fluence. For $\Delta T/T$, the maximum modulation ($\sim 4\times 10^{-3}$ for a laser heating fluence of 4 mJ/cm^2) was independent of film thickness for 200–800-Å films, to a first-order approximation. On the contrary, for $\Delta R/R$ the maximum modulation decreased from $\sim 4\times 10^{-3}$ to $\sim 1\times 10^{-3}$ for the 800-Å films.

We next discuss the shape of the thermomodulation from a qualitative point of view. The heating laser pulse interacts initially with free and bound electrons in the metal. For gold the Fermi level is ~ 2.4 eV above the top of the d band. Since our pump-probe wavelength is 615 nm, which corresponds to an energy of ~ 2 eV, then our pump is mainly interacting with free electrons. As explained previously, there exists an absorption tail below the band edge that extends as low as 1.7 eV in gold. Thus, at our laser wavelength there is also some interband absorption. In fact, the overwhelming evidence that the thermomodulation signal observed with femtosecond laser systems is due to the smearing of the Fermi distribution,[4,7] i.e., due to changes in the occupancy of states near the Fermi level as a result of electronic heating that modulates the dielectric constant. Consequently, the optical properties (as probed by transmissivity and reflectivity) is modulated. While the thermomodulation signals could result from other effects such as thermal expansion, enhanced electron-phonon interaction, and shifting of the Fermi level, these are thought to have only a relatively small contribution to the femtosecond thermomodulation signal. The magnitude of this contribution, however, is not well determined.

The initial fast thermomodulation signal is due to the electronic heating. Because of the low heat capacity of the electrons, they respond "instantaneously" to the laser field. During this fast heating of the electrons, the lattice remains very close to its initial temperature. The hot electrons generated by the laser field thermalize with each other by electron-electron collisions, transfer their energy to the lattice by electron-phonon collisions, and scatter at defects, impurities, and surfaces. The possibility of collective excitation of plasma oscillation is precluded since the plasma frequency corresponds to about the Fermi energy.[27] Thus, an electron-electron collision causes an excited electron to lose a large fraction of its energy. If we assume that electron-phonon collisions is the main mechanism by which the energy contained in the hot electrons is transferred to the lattice, then the fast transient signal decay time is related to the time needed

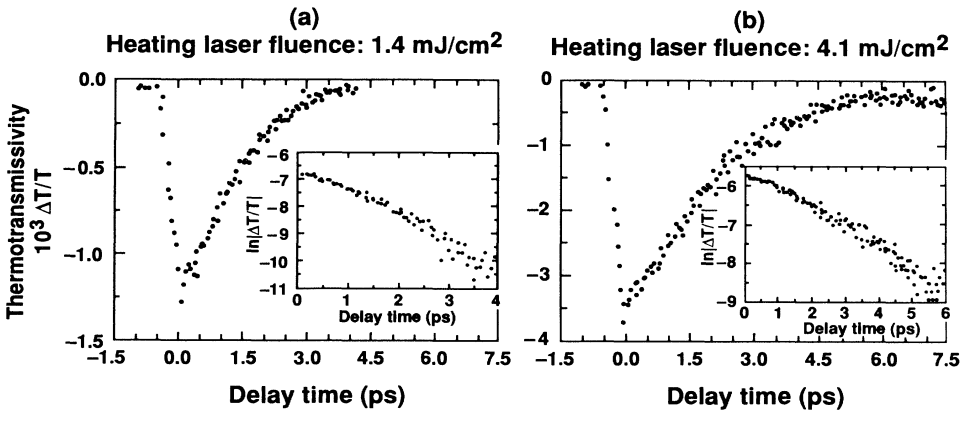

FIG. 2. Time-resolved thermomodulation transmissivity of 200-Å single-crystalline gold film taken with different heating laser fluences: (a) 1.4 mJ/cm^2, (b) 4.1 mJ/cm^2. The inset is a semilogarithmic plot of the fast transient decay.

for equilibrium to be established between the electrons and the phonons. The long tail, which persists in the thermomodulation signals for times that appear to be much longer than our probing time, can be explained by modulation of the optical properties as a result of simple heating of the metal as in conventional, i.e., slow thermomodulation spectroscopy.

While our experimentally measured quantities are those of the transient thermomodulation of the reflectivity and the transmissivity, these quantities are difficult to interpret in view of a change in the density of states near the Fermi level caused by electron heating. The measurement of the transient dielectric constant is more fundamental and lends itself to a clearer interpretation of nonequilibrium heating. The reflectivity and the transmissivity are related to the real and the imaginary parts of the dielectric constant through the Fresnel formula.[28] A derivation of this relation for an absorbing film deposited on a transparent substrate, and accounting for multiple reflection at the film-substrate interface was made by Abèles.[28] In thermomodulation, $\Delta R/R$ and $\Delta T/T$ result due to variations in ε_1 and ε_2. For a small modulation, these are related by[29]

$$\Delta R/R=\alpha_1\Delta\varepsilon_1+\alpha_2\Delta\varepsilon_2 , \quad (1)$$

$$\Delta T/T=\beta_1\Delta\varepsilon_1+\beta_2\Delta\varepsilon_2 , \quad (2)$$

where α_1, α_2, β_1 and β_2 are functions of ε_1 and ε_2, and can be obtained from the relationships derived by Abèles, which is listed in the Appendix. Knowing $\Delta R/R$ and $\Delta T/T$, we can then solve for $\Delta\varepsilon_1$ and $\Delta\varepsilon_2$.

This type of analysis is valid only if the sample is heated uniformly across its thickness; that is, if the hot electrons are geometrically confined because the sample thickness is less than or comparable to the skin depth. An example of this analysis is shown in Fig. 3. Displayed in Figs. 3(a) and 3(b) are the transient thermoreflectivity and thermotransmissivity for a 200-Å single-crystalline film. $\Delta R/R$ was obtained for a laser heating fluence of 3.33 mJ/cm^2, while $\Delta T/T$ was for a fluence of 2.96 mJ/cm^2. Since both $\Delta R/R$ and $\Delta T/T$ were directly proportional to the laser fluence, we have multiplied $\Delta T/T$ by a correction factor of 1.125 before performing the transformation to obtain the modulation in the dielectric constant. Solving for $\Delta\varepsilon_1$ and $\Delta\varepsilon_2$, we obtain the curves shown in Figs. 3(a) and 3(d). The following conclusions can be made regarding the transient modulation of the real and imaginary parts of the dielectric constant: (i) their temporal shape follows that of $\Delta R/R$ and $\Delta T/T$; (ii) the modulation in ε_2 is larger than that in ε_1 (peak $\Delta\varepsilon_2/\varepsilon_2=0.057$, while $\Delta\varepsilon_1/\varepsilon_1=0.017$); and (iii) $\Delta\varepsilon_2$ is positive indicating an enhancement of absorption during transient heating. It is well recognized that modulation to ε_2 represents modulation to the sum of all electronic transitions at the probe wavelength originating in different areas of momentum space. A notable feature of modulation experiments on gold is a derivative peak centered at $\sim$2.4 eV, which is attributed to transitions from the top of the d band to the Fermi level.[23,24] Electronic heating results in reducing (increasing) the number of occupied states below (above) the Fermi level. Since our probe wavelength corresponds to an energy of 2 eV, the experimentally observed enhanced absorption is consistent with that expected, due to electronic heating.

We next decompose the transient modulation in the thermoreflectivity and thermotransmissivity, each into two components related to the modulation of the real and the imaginary parts of the dielectric constant. The relative importance of these components is set by the magnitude of the coefficients α_1, α_2, β_1, and β_2 at the probe wavelength. For $\Delta R/R$, these components are $\alpha_1\Delta\varepsilon_1$ and $\alpha_2\Delta\varepsilon_2$; and for $\Delta T/T$ these are $\beta_1\Delta\varepsilon_1$ and $\beta_2\Delta\varepsilon_2$. Such a decomposition of $\Delta R/R$ and $\Delta T/T$ is shown in Fig. 4, from which we can conclude the following: (i) the modulation of ε_2 is dominant at the probe wavelength, $\lambda=615$ nm, and results in the negative sign for both $\Delta R/R$ and $\Delta T/T$, and (ii) the modulation of ε_1 results also in a negative sign for $\Delta R/R$, however, it results in a positive sign for $\Delta T/T$.

Inherent in the above analysis is the assumption of uniform heating across the thickness of the thin gold film. We justify this assumption by observing that the 200-Å films are comparable in thickness to the laser skin depth in gold at $\lambda=615$ nm and that electron transport can further distribute electronic heating along the thickness of

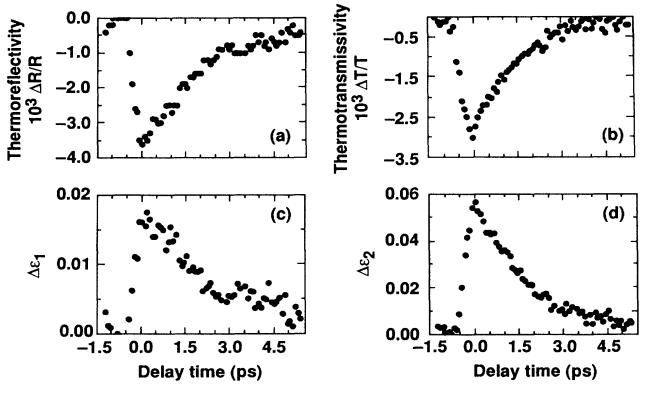

FIG. 3. Transient (a) thermoreflectivity $\Delta R/R$ and (b) thermotransmissivity $\Delta T/T$ of a 200-Å single-crystalline gold film. $\Delta R/R$ and $\Delta T/T$ are inverted to obtain the transient modulation to (c) the real, $\Delta\varepsilon_1$, and (d) imaginary, $\Delta\varepsilon_2$, parts of the dielectric constant.

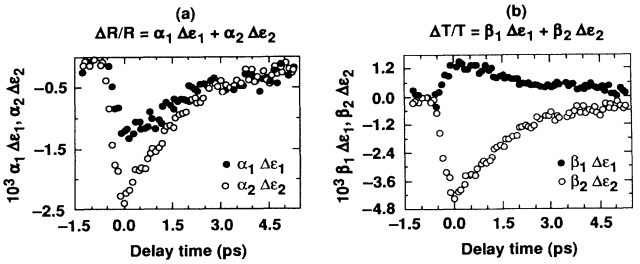

FIG. 4. Transient (a) thermoreflectivity $\Delta R/R$ and (b) thermotransmissivity $\Delta T/T$ after decomposing it into two components each related to the modulation of the real and imaginary parts of the dielectric constant.

the film. The degree by which this uniform heating assumption is violated depends on the film thickness and on the transport properties of the hot electrons.

IV. MODEL

The time evolution of the electron and the lattice effective temperatures, T_e and T_l, respectively, was previously described by a set of two coupled nonlinear partial differential equations:[1]

$$C_e(T_e)\frac{\partial T_e}{\partial t}=\nabla(\kappa\nabla T_e)-G(T_e-T_l)+P_0(r,t) \quad (3)$$

and

$$C_l\partial T_l/\partial t=G(T_e-T_l)\ , \quad (4)$$

where the electronic heat capacity per unit volume $C_e(T_e)$ is assumed to be proportional to the electron temperature, C_l is the lattice heat capacity per unit volume, κ is the electronic thermal conductivity, G is the electron-phonon coupling parameter, which is assumed a constant, and $P_0(r,t)$ represents laser power deposited in the sample. These equations include several assumptions, which could be violated to some degree and can render their validity questionable. We next discuss these assumptions and elaborate on how they could affect the validity of the above simple model.

Local equilibrium is assumed among each of the electron and the phonon subsystems; that is, electron-electron (Coulomb) collisions are assumed to maintain the electron subsystem as a Fermi-Dirac distribution at temperature T_e, while phonon-phonon (anharmonic) collisions are assumed to maintain the phonon distribution as a Bose-Einstein distribution characterized by the temperature T_l. These assumptions are certainly violated over some time or even over all of our probing time. The validity of these assumptions was previously considered by Agranat, Anisimov, and Makshantsev.[30] Following their analysis, the thermalization time of the electron subsystem, τ_e, can be estimated from the relation

$$1/\tau_e\sim v_F k_F(\langle E\rangle/E_F)^2\ , \quad (5)$$

where v_F is the Fermi velocity, k_F is the Fermi wave vector, E_F is the Fermi energy, and $\langle E\rangle$ is the mean electron energy in the metal determined from the Fermi level. For gold, $v_F=1.40\times10^8$ cm/s, $k_F=1.21\times10^8$ cm^{-1}, and $E_F=5.53$ eV. For a mean electron energy of 0.086 eV, which corresponds to 1000 K, the electron thermalization time, τ_e, is estimated to be $\sim$250 fs. Since a mean electron temperature of 1000 K is readily obtained at the laser fluences reported here, electron thermalization is expected to occur on a time scale comparable to the heating-laser-pulse width, which is significantly less than the electron-phonon relaxation time. Under these conditions, assigning a temperature to the hot electrons can be justified when considering times longer than several hundred femtoseconds. To be precise, we refer to T_e as an effective electron temperature since significant deviations from local equilibrium conditions could be present during the femtosecond laser heating pulse, and perhaps some deviation could be present afterwards.

A noteworthy experimental measurement of the hot-electron energy distribution is that of Fann *et al.*[10] In their experiment, the electron energy distribution in a 400-fs laser-heated gold film was directly measured using time-resolved photoemission. The temporal resolution of this experiment was $\sim$700 fs. Results showed that for all times above 800-fs delay between the heating pulse and the ultraviolet probe pulse, the measured hot-electron distribution can be well fitted to a Fermi-Dirac function. In these experiments, a laser heating fluence causing an effective peak electron temperature of several hundred degrees was used. While there was a reproducible deviation from a Fermi-Dirac function at early times, these represented only 10–50 % departure from the fit at delay times <800 fs and were not present for longer delay times. Thus, our assumption of an effective electron temperature in the simplified model of Eqs. (3) and (4), does not seem to be in large error for the present experimental conditions.

We next consider the phonon subsystem. Phonon-phonon equilibration occurs through scattering described by the anharmonic potential. The thermalization time of the phonons, $\tau_{\rm ph}$, can be estimated by the relation[30,31]

$$\tau_{\rm ph}\sim l_{\rm ph}/v_s\ , \quad (6)$$

where $l_{\rm ph}$ is the phonon mean free path, which depends on the phonon energy, and $v_s=3.7\times10^3$ m/s is the speed of sound in gold. For equilibrium conditions at temperature T, $l_{\rm ph}\sim Mv_s^2a/kT\gamma^2$, where $M=329\times10^{-27}$ kg is the ionic mass, $a=4\times10^{-10}$ m is a length of the order of the lattice constant, k is the Boltzmann constant, and $\gamma\sim2$ is the Gruneisen constant. Evaluating $\tau_{\rm ph}$ at $T=300$ K provides an upper limit on the phonon thermalization time. Using these conditions, $\tau_{\rm ph}$ is estimated to be of the order of 10^{-11} s, i.e., larger than the electron-phonon energy-loss lifetime. Thus, the phonon subsystem is expected to be out of equilibrium for times longer than $\tau_{e\text{-ph}}$. The validity of the simple analysis of nonequilibrium heating represented by Eqs. (3) and (4) depends on the degree of departure from equilibrium conditions. For the experiments we are presently reporting on, the initial temperature of the gold film was $\sim$300 K. The femtosecond heating pulse could not raise the lattice temperature by more than $\sim$40 K. That is, during electron-phonon relaxation, the phonon population can be described by two components; a large component represented by a temperature of $\sim$300 K, plus a small component of nonequilibrium phonons. Since the mean phonon temperature undergoes only a very small change by laser heating, it is reasonable to expect that, under these conditions, the deviation of the phonon subsystem from equilibrium would not significantly affect the electron-phonon decay and Eqs. (3) and (4) remain basically valid.

Another complication arises due to the nature of heat transport. In Eqs. (3) and (4), the electronic heat transport is assumed to be completely diffusive. The thermalized hot-electron population is assumed to diffuse to the bulk of the thin film due to the temperature gradient set between the laser-heated surface and the bulk of the sam-

ple. Femtosecond time-of-flight experiments have shown that hot-electron transport across 500–3000-Å gold films can proceed with a velocity approaching that of the Fermi velocity.[8] These measurements provided significant evidence of a ballistic component to electronic heat transport. The question of the nature of hot-electron transport in femtosecond experiments is still not well answered and it is reasonable to expect that ballistic and diffusive transport are both occurring. The importance of each of these mechanisms depends on the considered depth inside the film and on the mean free path of the initial hot electrons.

Considering the geometry of the 200-Å films (film thickness slightly over the skin depth), hot electrons are geometrically confined and electron diffusion perpendicular to the surface is negligible; that is, the film is heated uniformly. This is due to the fact that the optical skin depth in gold is ~ 150 Å at $\lambda = 615$ nm and that hot-electron transport can effectively distribute the energy uniformly throughout the thickness of the film. In addition, radial diffusion of the hot electrons is negligible at time scales of interest (a few picoseconds after the heating laser pulse). Such radial diffusion is very slow since the heating laser beam diameter is much larger than the optical skin depth. Therefore, for the 200-Å films, the diffusion term could be dropped out of Eq. (3).

Electron-defect collisions are not explicitly included in Eqs. (3) and (4). Elastic electron-defect collisions modifies the diffusion term due to electron momentum change after such a collision. Electron collisions with defects are also known to modify electron-electron[31–34] and electron-phonon coupling.[34–40] These effects, however, will be neglected for now. Subsequently, we will show that the effect of electron-defect collisions on hot-electron energy loss can be empirically accounted for by modifying the electron-phonon coupling constant, G.

If we neglect diffusion and electron-defect collisions, then a solution of Eqs. (3) and (4) indicates that, initially, the electron temperature could be raised by more than 1000 K, while the lattice temperature remains basically unaltered as shown in Fig. 5. In this example, Eqs. (3) and (4) were solved for $C_e(T_e) = 66T_e$ J/m^3 K, $C_l = 2.4 \times 10^6$ J/m^3 K,[41] a Gaussian heating laser pulse (150 fs full width at half maximum), 5% absorption, which was experimentally measured and assumed to be deposited uniformly across the thickness of the film, and neglecting electron transport. Comparison of Fig. 5(a) with Fig. 5(b) shows that $\tau_{e\text{-ph}}$ increases with the heating fluence. This is consistent with the thermomodulation results shown in Fig. 2. The physical reason for this increase in $\tau_{e\text{-ph}}$ is the linear dependence of the electronic heat capacity on the electron temperature. In the model shown in Fig. 5, we have assumed the electron-phonon coupling constant G to be 4×10^{16} W/m^3 K. This value seems to best fit the decay time in the thermomodulation signal that we observed for the 200-Å polycrystalline films. The comparison of the transient thermomodulation decay time with the hot-electron energy-loss lifetime should be interpreted in view of several uncertainties. These include the pump laser fluence, which depends on the laser focal spot (5 ± 1 μm), and in quantitatively relating the thermomodulation signal to hot-electron decay.

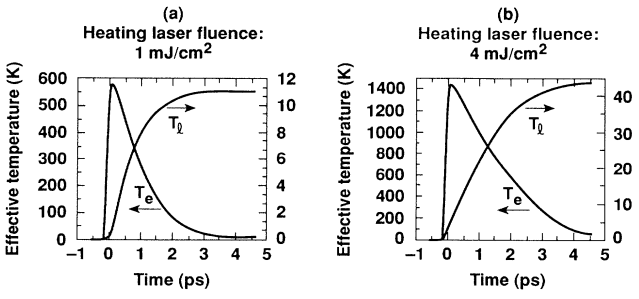

FIG. 5. Temporal evolution of the effective electron and lattice temperatures, T_e and T_l, as predicted by the nonequilibrium heating model of Eqs. (3) and (4). The model was solved for a 200-Å film with a laser heating fluence of (a) 1 mJ/cm^2 and (b) 4 mJ/cm^2.

An important question associated with the femtosecond time-resolved thermomodulation experiments is how to quantitatively relate the thermomodulation signal to an electron effective temperature. One approach is to derive the transient modulation in the real and the imaginary parts of the dielectric constant using, for example, the measured transient modulation in reflectivity and transmissivity. Once the transient dielectric constant is known, it can be related to the band structure and the optical transitions in order to obtain an effective electron temperature. This, however, requires precise knowledge of all optical transitions at the probe wavelength and the manner in which the changes in the occupancy of states due to electronic heating affect their probability. Unfortunately, this information is not available, especially when considering that our probe laser wavelength is ~ 0.4 eV off resonance with the top of the d band to the Fermi-level transition.

Taking these difficulties into account, we have previously proposed an empirical method of analyzing transient thermoreflectivity in order to obtain the transient effective electron temperature. Our proposed approach is based on deriving a differential thermomodulation "Fermi" function, which relates the electron-heating-induced thermomodulation to a unit electron temperature increase starting from a particular temperature. This differential Fermi function is obtained experimentally by performing transient thermomodulation at different ambient temperatures.[5] Simply put, a constant electron temperature jump induces a thermomodulation signal that is dependent on the initial temperature of the electrons. For gold probed at $\lambda \sim 615$ nm, the differential Fermi function was experimentally shown to decrease towards zero as the ambient temperature is reduced below ~ 150 K. Asymptotic behavior appears to be reached near an ambient temperature of 300 K. Higher temperatures were not considered in Ref. 5. The decay time of the transient thermomodulation signal can resemble that of hot-electron decay time if the considered temperature region for the differential Fermi function is constant, which appears to be the case for the lower heating fluences. At the higher fluences, where the effective electron tempera-

ture is raised by many hundreds of degrees above the ambient 300 K, asymptotic behavior of the differential Fermi function might not persist. The extent for which the thermomodulation decay could deviate from the hot-electron decay is not known. This represents an uncertainty in the interpretation of the thermomodulation data. We could, however, conclude that there seems to be a qualitative agreement between the hot-electron decay time and the thermomodulation decay time based on the above-mentioned asymptotic behavior of the differential Fermi function. Moreover, it is interesting to note that the electron-phonon coupling parameter G derived from fitting the transient-thermoreflectivity decay with hot-electron decay as derived from Eqs. (3) and (4) shows remarkable agreement with that theoretically predicted for several metals.[12]

Another experimental effect on the transient thermomodulation signal is caused by the finite pulse width of our probe. Therefore, our thermomodulation signal is, in fact, the result of the convolution of the actual signal with the probe pulse. This only affects the shape of the signal near its peak, where the decay rate is fastest. Since the transient thermomodulation decay signals are about an order of magnitude larger than our probe pulse width, we do not expect that this effect would cause significant error. This convolution effect, however, appears to be visible in the semilogarithmic plots in the inset of Fig. 1, where early in the decay ($\lesssim 0.5$ ps) there appears to be a deviation from the simple exponential that is subsequently observed.

V. DEPENDENCE OF HOT-ELECTRON DECAY TIME ON CRYSTAL STRUCTURE

In order to investigate the role of defects on hot-electron energy-loss lifetime, $\tau_{e\text{-ph}}$, we have conducted transient thermoreflectivity and thermotransmissivity on single-crystalline and polycrystalline 200-Å films. The decay time of the fast transient was measured as a function of the heating laser fluence. Results are shown in Fig. 6. Each datum is an average of 6–8 different measurements conducted using three sets of single-crystalline and polycrystalline films. The decay time is defined as the width of the transient signal at e^{-1} of the difference between the maximum transient and the slowly decaying tail following it. The standard deviation of the decay time measurements was less than 10% of the average value. Results clearly show a systematic, almost constant increase in the decay time for the single-crystalline films when compared with the polycrystalline films.

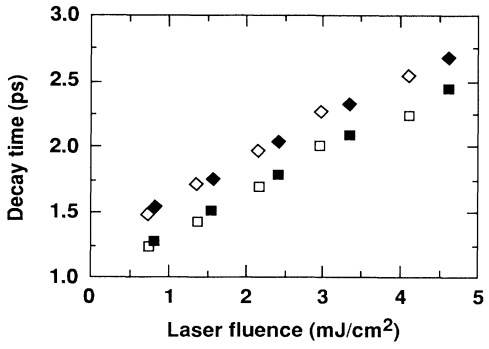

FIG. 6. Decay time of the fast transient in the thermoreflectivity (solid symbols) and thermotransmissivity (open symbols) of 200-Å single-crystalline (diamond) and polycrystalline (squares) gold films as a function of heating laser fluence.

Several film properties could have caused this deviation. First, the film thickness could be different, which would cause a difference in power deposition between the polycrystalline and single-crystalline films. This is ruled out since both types of films were fabricated using the same conditions, except for the substrate type and temperature. Thus, errors in the relative thickness of the different films is very small (within several angstroms). As described previously, the fabrication of the single-crystalline gold films involves their deposition on a thin layer of silver deposited on a sodium chloride crystal. Some of the gold could alloy with the silver and this alloyed layer would then be acid etched along with the silver during removal of the gold film. The reduction in the gold film thickness by alloying and subsequent removal is minimized by maintaining a relatively low substrate temperature during gold film deposition, ~450 K, to minimize alloying without adversely affecting epitaxy. More importantly, the thickness of the silver layer when depositing the 200-Å film was only ~10 Å. Thus, alloying and subsequent removal of the gold film could not have reduced the film thickness by more than that.

Second, the removal process of the single-crystalline films could have introduced some unexpected changes in film properties that might have an effect on hot-electron decay. This hypothesis was tested by conducting the transient thermomodulation measurements on polycrystalline films deposited on a sodium chloride crystal at room temperature and subsequently removed using the same technique employed for the single-crystalline films. Results for these polycrystalline films were in agreement with those directly deposited on the glass slide. Thus, the film lift-off process could not have been responsible for the observed difference between the two types of films.

Third, the optical properties of the polycrystalline and single-crystalline films could differ in a way that causes the power deposition to vary for the same incident laser fluence. The film that absorbs more laser energy will subsequently have a longer transient decay time. This was a major concern especially since published data on the optical properties of thin films are known to differ among themselves and the absolute value of thin-film absorption cannot be easily measured with high precision. To check for the magnitude of the variation in power deposition between the polycrystalline and single-crystalline films, we have compared the magnitude of the maximum modulation in the transmissivity for the two kinds of films at different pump fluences. For this comparison, the transient thermomodulation measurements for the two types of films were conducted immediately, one after the other, to avoid changes in the laser heating fluence. Three independent measurements were made for each fluence

(four different fluences ranging from 0.7 to 4 mJ/cm^2 were considered). The peak thermomodulation transmissivity signal for the polycrystalline and single-crystalline films showed better than 5% agreement, with the modulation signal leaning towards being slightly higher for the polycrystalline films. This seems to preclude the possibility that the difference in the observed decay time between the polycrystalline and single-crystalline films is due to power deposition effects.

This leads us to the conclusion that the shorter transient thermomodulation decay time observed for the polycrystalline films is due to faster hot-electron energy loss (smaller $\tau_{e\text{-ph}}$), which is promoted by an increased level of defects. Several theoretical studies have shown that defects can influence $\tau_{e\text{-ph}}$ by affecting the rate of energy transfer between electrons and phonons. Gold has a monatomic unit cell, therefore, there are no optical phonons. An increased level of defects promotes coupling between electrons and transverse acoustic phonons due to partial removal of crystal momentum conservation constraints by intermediate impurity scattering.[36] In contrast, ultrasonic attenuation experiments and theoretical calculations have shown that coupling between electrons and longitudinal phonons is reduced with increased level of defects.[38] This was explained by observing that the longitudinal vibrations, which the electrons fluctuate in phase with, set up regions of compressed electron gas with increased mean energy and others with dilated electron gas with reduced mean energy. Energy is dissipated from the longitudinal vibration by electron diffusion from the high-energy to the low-energy region. This diffusion is hindered by disorder, thus, electron-phonon coupling is reduced.[38] This effect, however, does not apply to our case, since it treats the case where the phonons are externally heated and subsequently come to equilibrium with the electrons (i.e., the inverse of our case). Therefore, the intermediate defect scattering is expected to reduce the hot-electron energy-loss lifetime.

We next briefly comment on the nature of electron-lattice defect collisions for the two different types of gold films used in our experiments. Each individual electron undergoes a collision with another electron or a phonon on the average within a mean free path. For a 2-eV hot electron, the mean free path for an electron-electron collision or an electron-phonon collision is about a few hundred angstroms. For the polycrystalline gold films used in the present experiments, microstructural examination revealed a large distribution of grain sizes with an estimated average of $\sim$155 Å. Thus, the number of electron–grain boundary collisions is comparable to, or even larger than, that of electron-electron and electron-phonon collisions. Grain boundaries are known to be very efficient in scattering conduction electrons. For metals, the probability of an electron to pass a single grain boundary is theoretically estimated to be about 0.7.[42] Given that each hot electron undergoes several collisions with grain boundaries prior to thermalization with the lattice, then grain boundaries could be responsible for the observed difference in the decay time between the polycrystalline and the single-crystalline films. Other defects such as dislocations or stacking faults, which are present in the single-crystalline films, are known to be significantly less effective in scattering conduction electrons.[43] The scattering of conduction electrons by stacking faults in Cu was theoretically calculated.[44] At nearly all wave vectors, conduction electrons at the Fermi surface penetrates a stacking fault with a very small probability of scattering (10^{-3}–10^{-4}). Thus, stacking faults represent a very weak perturbation to conduction electrons near the Fermi level.[44]

For the 200-Å films, the average grain size is comparable to the film thickness and it is difficult to separate the role of lattice defects on hot-electron energy-loss lifetime from that of surfaces. Previous studies on the resistivity of thin films has indicated that the surface roughness of polycrystalline gold films causes the diffuse scattering of electrons at the surface. This is in contrast to the atomically smooth nature of the surface of single-crystalline gold films which specularly reflects the electrons.[21] From a theoretical point of view, electron collisions with surfaces distort their momentum distribution in a manner that could depend on surface roughness.[45] Such surface effects were shown to penetrate into the interior a depth comparable to the mean free pass of the electrons[45] (i.e., throughout the thickness of the film). We have also conducted transient optical thermomodulation measurements on 100-Å polycrystalline and single-crystalline (epitaxially grown) films. For these films, electron microscopy showed the formation of separate islands that are interconnected by bridges with voids covering a significant area of the sample for both types of films. Similar trends were observed as for the 200-Å films.

We next compare the experimentally obtained transient decay time in Fig. 6 with the energy-loss lifetime, $\tau_{e\text{-ph}}$, obtained from the simple model of Eqs. (3) and (4). In the experimental measurements, we define the decay time as the width of the transient signal at e^{-1} of the difference between the maximum transient and the slowly decaying tail following it. For the model we define the $\tau_{e\text{-ph}}$ as the width of the transient electron temperature at e^{-1} of the difference between the peak T_e and its final equilibrium value. These definitions are made here mainly to facilitate a comparison of the results for single-crystalline versus polycrystalline films. In Fig. 7, the

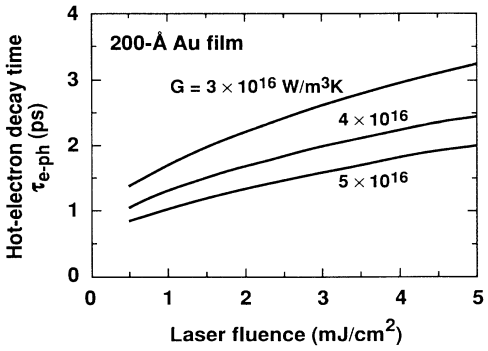

FIG. 7. Hot-electron energy-loss lifetime, $\tau_{e\text{-ph}}$, obtained from Eqs. (3) and (4) for the experimental conditions of Fig. 6.

theoretical $\tau_{e\text{-ph}}$ is shown as a function of laser fluence for different values of the electron-phonon coupling parameter, G. Comparison of Fig. 6 with Fig. 7, shows that the model predicts well the experimentally observed increase in decay time with laser fluence. Moreover, the solution of the model for $G=4\times10^{16}$ W/m^3 K shows agreement with the experimental transient decay time in the 200-Å polycrystalline films. For the single-crystalline films, comparison of the model with the experimental decay time indicates a small decrease in the electron-phonon coupling parameter from that for the polycrystalline film, $G\sim3.5\times10^{16}$ W/m^3 K.

VI. THE EFFECT OF CRYSTAL STRUCTURE ON ELECTRON TRANSPORT

The use of 200-Å films results in the geometric confinement of the hot electrons and thus allows the observation of the transient thermomodulation signal due to hot-electron energy loss without being affected by transport. For thicker films, hot-electron transport affects the thermomodulation signal. Therefore, the effect of lattice defects on hot-electron transport can be studied using thicker polycrystalline and single-crystalline films. We have conducted transient thermoreflectivity and thermotransmissivity on 400- and 800-Å polycrystalline and single-crystalline gold films. The decay time of the transient $\Delta R/R$ for single-crystalline films with different film thicknesses is shown in Fig. 8. We observe that as the film thickness is increased from 200 to 400 Å, there is a significant reduction (about a factor of 2) in the decay time. With the further increase in thickness to 800 Å, the reduction in the decay time is less. This shows that, for film thicknesses larger than the optical skin depth, the decay of the transient $\Delta R/R$ represents both hot-electron energy loss and electron transport inside the sample where it is not being probed by reflectivity.

We next consider the transient thermomodulation for the 800-Å single-crystalline and polycrystalline films. The results, displayed in Fig. 9, represent an average of 4–6 different measurements conducted on one set of films. The standard deviation in each decay time measurement is less 12% of the average value. Comparison

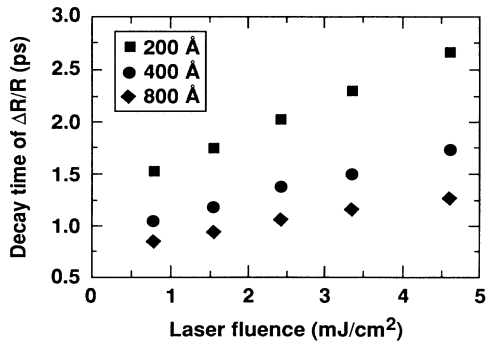

FIG. 8. Decay time of the fast transient in the thermoreflectivity as a function of laser heating fluence measured for film thicknesses of 200, 400, and 800 Å.

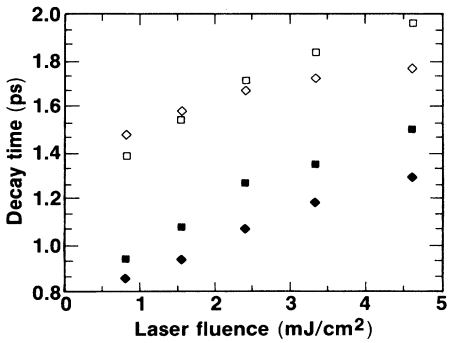

FIG. 9. Decay time of the fast transient in the thermoreflectivity (solid symbols) and thermotransmissivity (open symbols) of 800-Å single-crystalline (diamond) and polycrystalline (squares) gold films as a function of heating laser fluence.

of the results in Fig. 9 with that in Fig. 6 show that the transient decay time of $\Delta T/T$ is affected less by the increased film thickness than that of $\Delta R/R$ since reflectivity is influenced by each electron leaving the excited volume; whereas in a gross sense, transmissivity is influenced only by those electrons which leave (laterally) the volume associated with the probe beam path through the sample. This is a small effect since the diameter of the laser beam is much larger than both the optical skin depth and the film thickness.

For the 800-Å films, comparison of the transient thermoreflectivity for the polycrystalline films to those for the single-crystalline shows behavior opposite from that observed for the 200-Å films. The decay time of $\Delta R/R$ was faster for the single crystalline. We interpret these results by observing that, for the 800-Å films, hot-electron transport is impeded by grain boundaries. While grain boundaries increase electron-phonon coupling, this effect on transient $\Delta R/R$ decay time (which would cause it to decrease for the polycrystalline films) appears to be smaller than the opposite effect of impeding electron transport inside the film.

The thermal conductivity of metals is predominantly controlled by electron transport properties. The reduction of the thermal conductivity of metals by lattice defects is well demonstrated and is attributed to the reduction of electron mean free path. Previous transient thermomodulation studies have shown that the thermal diffusivity, defined as the ratio of the thermal conductivity to the heat capacity per unit volume, of evaporated and sputtered metal films can be significantly less than that of bulk materials. The thermal diffusivity of nickel thin films was reduced from its bulk value by a factor of 3 for an evaporated film and by a factor of 4 for a sputtered film.[46]

In Fig. 9, an interesting sign reversal is observed in the difference between the decay time of the fast transient in $\Delta T/T$ for the polycrystalline and single-crystalline films as a function of laser fluence. This was also observed for 400-Å films. At this stage we can only offer the following qualitative explanation. We notice that $\Delta T/T$ is less affected by electron transport than $\Delta R/R$ and that hot-

electron transport competes with energy loss. For low laser fluences, where diffusion is less important, the increased electron-phonon coupling for the polycrystalline films results in a faster decay as observed for the 200-Å films. At the higher fluences diffusion becomes more important. This affects the spatial distribution of hot electrons across the film, causing it to be less uniform for the polycrystalline than for the single-crystalline films due to lower κ. Since the hot-electron energy-loss lifetime increases with the effective electron temperature, we would expect a slower transient decay time for the polycrystalline films. A quantitative analysis of electron transport would require a more extended treatment than that permitted by the diffusion term in Eq. (3). Among the factors which need to be considered are the possible role of ballistic hot-electron transport, the dependence of electron transport on T_e and T_l, and the nature of electron-lattice defects collisions.

We next make a brief comment on these factors and show that a much more complicated treatment is needed to model electron transport in the thicker films. The possibility of ballistic electron transport across the sample provides an uncertainty to Eqs. (3) and (4). In the femtosecond time-of-flight experiment of Ref. 8, heat transient time was clearly shown to scale linearly with sample thickness and to travel across the thickness of the sample with a velocity close to the Fermi velocity. This gives a strong evidence of a ballistic component to heat flow; however, as discussed in Ref. 8, femtosecond time-of-flight measurements by themselves do not provide a conclusive evidence of ballistic transport, since electron cooling and the dependence of the electronic thermal conductivity on temperature at large temperature excursions complicate the analysis. The relative magnitude of ballistic versus diffusive heat transport is not easily determined and requires further studies. A key parameter to better understanding this question is consideration of the available data on the range of hot electrons in gold. This represents a combined mean free path of electron-electron and electron-phonon scattering. The range of hot electrons in gold was previously measured as a function of hot-electron energy.[27] For 2-eV electrons, measured from the Fermi level, E_F, the range was 250±30 Å. This increased to about 650 Å for 1-eV electrons. The electron-phonon mean free path slowly increases with electron energy, E, according to $l_{e\text{-ph}} \sim (E+E_F)^2$ and is inversely proportional to the lattice temperature.[47] For gold $l_{e\text{-ph}}$ is about 200 Å for a 1–2-eV hot electron in a thermal phonon bath at 300 K.[27] For electrons close to the Fermi level, the electron-electron mean free path strongly depends on the electron energy according to $l_{e\text{-}e} \sim E^2$.[48] For 2-eV electrons, $l_{e\text{-}e}$ is estimated to be several hundred angstroms.[27,49] Since the 800-Å films are thicker than the range of a 2-eV hot electron, it is reasonable to expect that there is both a diffusive and a ballistic component to electron transport.

We next consider the dependence of the thermal conductivity on the effective electron and lattice temperatures. The thermal conduction of metals is dominated by electron transport. In the diffusive transport limit, the kinetic theory of gases indicates that the thermal conductivity is described by the relation

$$\kappa = \frac{1}{W} = \frac{1}{3} v l C_v = \frac{1}{3} v^2 \tau C_v \ , \tag{7}$$

where W is the thermal resistance, C_v is the heat capacity per unit volume, which is directly proportional to the electron temperature, v is the average electron velocity, τ is the average time between collisions, and l is the mean free path between collisions. Electron-electron, electron-phonon, and electron-imperfection collisions determine l and τ, and consequently κ and W. For a conduction electron with a low-excitation energy above the Fermi level, the exclusion principle reduces the probability of an electron-electron collision, thus τ is predominantly limited by electron-phonon collisions. Under these conditions τ is inversely proportional to the lattice temperature, to a first-order approximation. Thus, the thermal resistivity due to electron-phonon collisions will have the dependence $W_{e\text{-ph}} \sim T_l / T_e$. However, in the present experiments lattice heating is only a small fraction of the initial sample temperature. Thus, the effect of electronic heating on the electron conductivity could be important. An excited electron with energy E above the Fermi level in a metal with an effective electronic temperature T_e has an electron-electron scattering rate $1/\tau_{e\text{-}e}$ of the form

$$1/\tau_{e\text{-}e} = aE^2 + b(k_B T_e)^2 \ , \tag{8}$$

where k_B is the Boltzmann constant and a and b are independent of E and T_e.[50] If we assume that the electrons reach a state of quasiequilibrium among themselves, establishing an effective temperature $T_e \sim 1000$ K, then the scattering rate assumes the form $1/\tau_{e\text{-}e} \sim T_e^2$. Since the electronic heat capacity is directly proportional to the electron temperature, it follows that the electronic thermal resistivity due to electron-electron collisions, $W_{e\text{-}e}$, is proportional to T_e. Electron-defects collisions could also depend on T_e and T_l in a manner that is not presently understood and introduces an extra contribution to the thermal resistivity, $W_{e\text{-}i}$. If we assume that the collision rates due to the separate mechanisms can add up in accordance with the Matthiessen's role, then the thermal resistivity, W, is the sum of $W_{e\text{-}e}$, $W_{e\text{-ph}}$, and $W_{e\text{-}i}$. While the dependence of $W_{e\text{-}e}$ and $W_{e\text{-ph}}$ on T_e and T_l is qualitatively understood, the quantitative contribution of each of these scattering mechanisms to W is not presently available for the case of nonequilibrium heating. Therefore, even if we assume the diffusive limit, it is difficult to proceed further with this type of analysis in order to quantitatively model hot-electron relaxation in the thicker films using Eqs. (3) and (4).

VII. CONCLUDING REMARKS

We have conducted femtosecond time-resolved thermoreflectivity and thermotransmissivity on single-crystalline and polycrystalline thin gold films. The transient decay time for the reflectivity and the transmissivity are equal for film thicknesses comparable to the optical skin depth. For thicker films, a faster reflectivity decay time is observed due to hot-electron transport. Grain

boundaries, and perhaps surface roughness, in the polycrystalline films seem to slightly reduce the transient decay time, which is modeled by a small increase in the value of the electron-phonon coupling constant. Grain boundaries also appear to impede hot-electron transport which, for the thicker films, results in a slower decay time for the polycrystalline films.

We have shown that the technique of femtosecond transient thermotransmissivity and thermoreflectivity can be used to study the effect of lattice defects on hot-electron energy loss and transport in metals. This technique provides a powerful tool to characterize the nature of electron interaction with various types of lattice defects. Using samples with controlled and well-characterized density of structural defects or impurities, it will be possible to study their effect on the strength of the electron-phonon coupling. Time-resolved thermomodulation also offers the possibility to probe how electron transport is affected by a particular type of defect or impurity. The time-of-flight experiment outlined in Ref. 8 provides a particularly attractive geometry for transport studies. Quantitative measurements on the strength of the thermomodulation signal and relating it to the number of electrons arriving at the back surface would provide significant information on the scattering strength of a particular lattice defect, such as grain boundaries. The initial hot-electron energy, measured from the Fermi level, could be varied using a tunable femtosecond pump laser. These types of experiments would provide the data needed to compare with present theoretical understanding on the probability of electron scattering at various types of defects.[41–44]

ACKNOWLEDGMENTS

We would like to acknowledge G. O. Smith for assisting in the laser pump-probe experiments, H. Mizes of Xerox, Webster, for performing the atomic force microscopy, and W. E. Bron for helpful discussions. The work conducted at The University of Rochester was supported in part by the U. S. Department of Energy under Contract No. DE-FG02-88ER45376.

APPENDIX

The modulation of the real and the imaginary parts of the dielectric function, $\Delta\varepsilon_1$ and $\Delta\varepsilon_2$, is determined from the data on $\Delta R/R$ and $\Delta T/T$ as a function of time by considering the appropriate transformation. The complex index of refraction, $N=n+ik$, is related to the complex dielectric function by $N^2=\varepsilon_1+i\varepsilon_2$. We use the formulas derived by Abèles, which is a derivation of the Fresnel equations for an absorbing media on a transparent substrate. Multiple reflections at the metal-substrate interface are accounted for. If we define $n_0=1$ and $n_s=1.5$ to be the index of refraction of air and glass, d is the gold film thickness, λ is laser wavelength, then the reflection and the transmission from the metal side are given by[28]

$$R=\frac{abe^{2k\eta}+cde^{-2k\eta}+2r\cos 2n\eta+2s\sin 2n\eta}{bde^{2k\eta}+ace^{-2k\eta}+2t\cos 2n\eta+2u\sin 2n\eta},$$

$$T=\frac{16n_0n_s(n^2+k^2)}{bde^{2k\eta}+ace^{-2k\eta}+2t\cos 2n\eta+2u\sin 2n\eta},$$

where

$$\eta=2\pi d/\lambda,$$

$$a=(n-n_0)^2+k^2,\quad b=(n+n_s)^2+k^2,$$

$$c=(n-n_s)^2+k^2,\quad d=(n+n_0)^2+k^2,$$

$$s=2k(n_s-n_0)(n^2+k^2+n_0n_s),$$

$$u=2k(n_s+n_0)(n^2+k^2-n_0n_s),$$

$$r=(n_0^2+n_s^2)(n^2+k^2)-(n^2+k^2)^2-n_0^2n_s^2-4n_0n_sk^2,$$

$$t=(n_0^2+n_s^2)(n^2+k^2)-(n^2+k^2)^2-n_0^2n_s^2+4n_0n_sk^2.$$

Starting from the values of n and κ, or equivalently ε_1 and ε_2, it is possible to use the above equations to derive R and T. For our 200-Å gold films we measure $R=0.665\pm0.02$, while $T=0.28\pm0.02$. Since we can measure R and T for our samples, we can iterate through the above equations to obtain n and k. For example, for $n=0.19$ and $k=3.85$, we obtain $R=0.658$ and $T=0.273$, which is within our measurement accuracy. The published values of n and k are 0.21 and 3.272, respectively. We have found that our solutions for n and k are quite sensitive to the accuracy of the film thickness which is known only to ±50 Å. This might contribute to the difference between our derived n and k and the previously published values. Moreover, the optical properties of thin films are known to depend on thickness and are sensitive to film preparation. Nevertheless, deviations in our derived values of n and k from the published data could only have a small effect on the calculated $\Delta\varepsilon_1$ and $\Delta\varepsilon_2$. In proceeding with the analysis, we used the published values of n and k.

In thermomodulation, $\Delta R/R$ and $\Delta T/T$ result due to modulations in ε_1 and ε_2. These can be related by

$$\Delta R/R=\alpha_1\Delta\varepsilon_1+\alpha_2\Delta\varepsilon_2,$$

$$\Delta T/T=\beta_1\Delta\varepsilon_1+\beta_2\Delta\varepsilon_2,$$

where α_1, α_2, β_1, and β_2 are obtained from the above relationships derived by Abèles. Knowing $\Delta R/R$ and $\Delta T/T$, we can then solve for $\Delta\varepsilon_1$ and $\Delta\varepsilon_2$.

*Present address: Department of Electrical and Computer Engineering, Old Dominion University, Norfolk, VA 23529-0246.

[1]S. I. Anisimov, B. L. Kapeliovich, and T. L. Perelman, Zh. Eksp. Teor. Fiz. **66**, 776 (1974) [Sov. Phys. JETP **39**, 375 (1974)].

[2]M. I. Kaganov, I. M. Lifshitz, and L. V. Tanatarov, Zh. Eksp. Teor. Fiz. **31**, 232 (1956) [Sov. Phys. JETP **4**, 173 (1957)].

[3]M. L. Roukes, M. R. Freeman, R. S. Germain, R. C. Richardson, and M. B. Ketchen, Phys. Rev. Lett. **55**, 422 (1985).
[4]G. L. Eesley, Phys. Rev. Lett. **51**, 2140 (1983); Phys. Rev. B **33**, 2144 (1986).
[5]H. E. Elsayed-Ali, T. Juhasz, X. H. Hu, and W. E. Bron, *Quantum Electronics & Laser Science,* 1991 Technical Digest Series (Optical Society of America, Washington, DC, 1991), pp. 189–199; T. Juhasz, H. E. Elsayed-Ali, X. H. Hu, and W. E. Bron, Phys. Rev. B **45**, 13 819 (1992).
[6]H. E. Elsayed-Ali, T. B. Norris, M. A. Pessot, and G. A. Mourou, Phys. Rev. Lett. **58**, 1212 (1987).
[7]R. W. Schoenlein, W. Z. Lin, J. G. Fujimoto, and G. L. Eesley, Phys. Rev. Lett. **58**, 1680 (1987).
[8]S. D. Brorson, J. G. Fujimoto, and E. P. Ippen, Phys. Rev. Lett. **59**, 1962 (1987).
[9]J. G. Fujimoto, J. M. Liu, E. P. Ippen, and N. Bloembergen, Phys. Rev. Lett. **53** 1837 (1984).
[10]W. S. Fann, R. H. Storz, and J. Bokor, *Quantum Electronics & Laser Science,* 1991 Technical Digest Series (Optical Society of America, Washington, DC, 1991), pp. 16–18; and W. S. Fann, R. Storz, H. W. K. Tom, and J. Bokor, Phys. Rev. Lett. **68**, 2834 (1992).
[11]R. H. M. Groeneveld, R. Spirk, and A. Lagendijk, Phys. Rev. Lett. **64**, 784 (1990).
[12]S. D. Brorson, A. Kazeroonian, J. S. Moodera, D. W. Face, T. K. Cheng, E. P. Ippen, M. S. Dresselhaus, and G. Dresselhaus, Phys. Rev. Lett. **64**, 2172 (1990).
[13]P. B. Allen, Phys. Rev. Lett. **59**, 1460 (1987).
[14]K. M. Yoo, X. M. Zhao, M. Siddique, R. R. Alfano, D. P. Osterman, M. Radparvar, and J. Cunniff, Appl. Phys. Lett. **56**, 1908 (1990).
[15]P. B. Corkum, F. Brunel, N. K. Sherman, and T. Srinivasan-Rao, Phys. Rev. Lett. **61**, 2886 (1988).
[16]Comment by H. E. Elsayed-Ali, Phys. Rev. Lett. **64**, 1846 (1990). Reply by P. B. Corkum, F. Brunel, N. K. Sherman, and T. Srinivasan-Rao, *ibid.* **64**, 1847 (1990).
[17]J. A. Prybyla, T. F. Heinz, J. A. Misewich, M. M. T. Loy, and J. H. Glownia, Phys. Rev. Lett. **64**, 1537 (1990).
[18]F. Budde, T. F. Heinz, M. M. T. Loy, J. A. Misewich, F. de Rougemont, and H. Zacharias, Phys. Rev. Lett. **66**, 3024 (1991).
[19]H. E. Elsayed-Ali, T. Juhasz, G. O. Smith, and W. E. Bron, Phys. Rev. B **43**, 4488 (1991).
[20]G. A. Bassett, J. W. Menter, and D. W. Pashley, in *Structure and Properties of Thin Films,* edited by C. A. Neugebauer, J. B. Newkirk, and D. A. Vermilyea (Wiley, New York, 1959), p. 11.
[21]K. L. Chopra, L. C. Bobb, and M. H. Francombe, J. Appl. Phys. **34**, 1699 (1963).
[22]T. Juhasz, G. O. Smith, S. M. Mehta, K. Harris, and W. E. Bron, IEEE J. Quantum Electron. **QE-25**, 1704 (1989).
[23]R. Rosei and D. W. Lynch, Phys. Rev. B **5**, 3883 (1972).
[24]M. Cardona, *Modulation Spectroscopy, Solid State Physics Supplement 11* (Academic, New York, 1969).
[25]N. E. Christensen and B. O. Seraphin, Phys. Rev. B **4**, 3321 (1971).
[26]P. B. Johnson and R. W. Christy, Phys. Rev. B **6**, 4370 (1972); R. T. Phillips, J. Phys. D **16**, 489 (1983), and references therein.
[27]S. M. Sze, J. L. Moll, and T. Sugano, Solid-State Electron. **7**, 509 (1964).
[28]F. Abèles, in *Advanced Optical Techniques,* edited by A. C. S. Van Heel (North-Holland, Amsterdam, 1967), Chap. 5, p. 144.
[29]*Optical Properties of Solids: New Developments,* edited by B. O. Seraphin (North-Holland, Amsterdam, 1976), Chap. 4.
[30]M. B. Agranat, S. I. Anisimov, and B. I. Makshantsev, Appl. Phys. B **47**, 209 (1988).
[31]J. M. Ziman, *Principles of the Theory of Solids* (Cambridge University Press, Cambridge, 1964), Chap. 7, p. 205.
[32]E. Abrahams, P. W. Anderson, P. A. Lee, and T. V. Ramakrishnan, Phys. Rev. B **24**, 6783 (1981).
[33]G. Bergmann, Phys. Rep. **107**, 1 (1984).
[34]B. L. Altshuler, A. G. Aronov, and P. A. Lee, Phys. Rev. Lett. **44**, 1288 (1980).
[35]G. Bergmann, Phys. Lett. **29A**, 492 (1969).
[36]G. Bergmann, Phys. Rev. B **3**, 3797 (1971).
[37]D. Belitz, A. Gold, and W. Götze, Z. Phys. B **44**, 273 (1981).
[38]B. Keck and A. Schmid, J. Low Tem. Phys. **24**, 611 (1976).
[39]A. Schmid, Z. Phys. **259**, 421 (1973).
[40]H. Takayama, Z. Phys. **263**, 329 (1973).
[41]*American Institute of Physics Handbook,* 3rd ed., edited by D. E. Gray (McGraw-Hill, New York, 1972).
[42]G. Reiss, J. Vancea, and H. Hoffmann, Phys. Rev. Lett. **56**, 2100 (1986).
[43]See, e.g., J. M. Ziman, *Electrons and Phonons* (Clarendon, Oxford, 1962), Chap. 6.
[44]H. Bross, J. Phys. F **12**, 2883 (1982).
[45]E. A. Stern, Phys. Rev. **162**, 565 (1967).
[46]C. A. Paddock and G. L. Eesley, J. Appl. Phys. **60**, 285 (1986).
[47]A. H. Wilson, *The Theory of Metals* (Cambridge University Press, Cambridge, 1954), p. 264.
[48]J. J. Quinn, Phys. Rev. **126**, 1453 (1962).
[49]W. F. Krolikowski and W. E. Spicer, Phys. Rev. B **1**, 478 (1970).
[50]N. W. Ashcroft and N. D. Mermin, *Solid State Physics* (Holt, Rinehart and Winston, Philadelphia, PA, 1976), Chap. 17, p. 347.

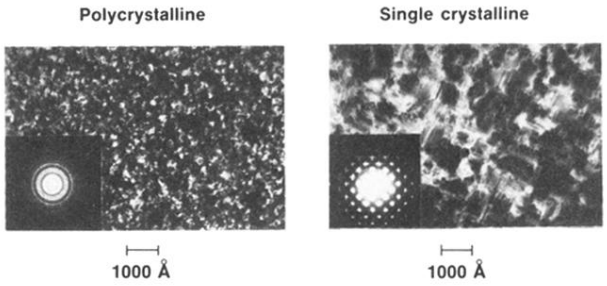

FIG. 1. Transmission electron micrographs and electron diffraction patterns of polycrystalline and single-crystalline gold films.